ISSN 1674-1056
http://cpb.iphy.ac.cn
http://iopscience.iop.org/cpb
中国物理 B
Chinese Physics
中国物理 Chinese Physics B

$CsPbBr_3$ nanocrystal for mode-locking Tm-doped fiber laser

Yan Zhou(周延), Renli Zhang(张仁栗), Xia Li(李夏), Peiwen Kuan(关珮雯), Dongyu He(贺冬钰), Jingshan Hou(侯京山), Yufeng Liu(刘玉峰), Yongzheng Fang(房永征), Meisong Liao(廖梅松)
Citation: Chin. Phys. B . 2019, 28(9): 094203 . **doi:** 10.1088/1674-1056/28/9/094203
Journal homepage: http://cpb.iphy.ac.cn; http://iopscience.iop.org/cpb

What follows is a list of articles you may be interested in

Zinc-oxide nanoparticle-based saturable absorber deposited by simple evaporation technique for Q-switched fiber laser

Syarifah Aloyah Syed Husin, Farah Diana Muhammad, Che Azurahanim Che Abdullah, Siti Huzaimah Ribut, Mohd Zamani Zulkifli, Mohd Adzir Mahdi
Chin. Phys. B . 2019, 28(8): 084207 . **doi:** 10.1088/1674-1056/28/8/084207

Polymer waveguide thermo-optical switch with loss compensation based on $NaYF_4$: 18% Yb^{3+}, 2% Er^{3+}nanocrystals

Gui-Chao Xing(邢桂超), Mei-Ling Zhang(张美玲), Tong-He Sun(孙潼鹤), Yue-Wu Fu(符越吾), Ya-Li Huang(黄雅莉), Jian Shao(邵健), Jing-Rong Liu(刘静蓉), Fei Wang(王菲), Da-Ming Zhang(张大明)
Chin. Phys. B . 2018, 27(11): 114218 . **doi:** 10.1088/1674-1056/27/11/114218

Observation of self-Q-switching in bulk Yb: GdYSiO laser

Shuang Gong(公爽), Jin-Rong Tian(田金荣), He-Yang Guo Yu(郭于鹤洋), Zi-Kai Dong(董自凯), Chang-Xing Xu(许昌兴), Wen-Ping Zhang(张文平), Yan-Rong Song(宋晏蓉)
Chin. Phys. B . 2018, 27(4): 044202 . **doi:** 10.1088/1674-1056/27/4/044202

Spectral dynamical behavior in two-section, quantum well, mode-locked laser at 1.064μm

Si-Hang Wei(魏思航), Ben Ma(马奔), Ze-Sheng Chen(陈泽升), Yong-Ping Liao(廖永平), Hong-Yue Hao(郝宏玥), Yu Zhang(张宇), Hai-Qiao Ni(倪海桥), Zhi-Chuan Niu(牛智川)
Chin. Phys. B . 2017, 26(7): 074208 . **doi:** 10.1088/1674-1056/26/7/074208

Confinement-induced nanocrystal alignment of conjugated polymer by the soft-stamped nanoimprint lithography

Li Xiao-Hui, Yu Ji-Cheng, Lu Nai-Yan, Zhang Wei-Dong, Weng Yu-Yan, Gu Zhen
Chin. Phys. B . 2015, 24(10): 104215 . **doi:** 10.1088/1674-1056/24/10/104215

$CsPbBr_3$ nanocrystal for mode-locking Tm-doped fiber laser*

Yan Zhou(周延)[1], Renli Zhang(张仁栗)[2], Xia Li(李夏)[2], Peiwen Kuan(关珮雯)[2], Dongyu He(贺冬钰)[3], Jingshan Hou(侯京山)[3], Yufeng Liu(刘玉峰)[3], Yongzheng Fang(房永征)[3,†], and Meisong Liao(廖梅松)[2,‡]

[1] *School of Science, Shanghai Institute of Technology, Shanghai* 201418, *China*

[2] *Key Laboratory of Materials for High Power Laser, Shanghai Institute of Optics and Fine Mechanics, Chinese Academy of Sciences, Shanghai* 201800, *China*

[3] *School of Materials Science and Engineering, Shanghai Institute of Technology, Shanghai* 201418, *China*

(Received 18 March 2019; revised manuscript received 9 June 2019; published online 7 August 2019)

$CsPbBr_3$ nanocrystal is used as the saturable absorber (SA) for mode-locking Tm-doped fiber laser in a ring fiber cavity. The modulation depth, saturable intensity, and non-saturable loss of the fabricated SA are 14.1%, 2.5 MW/cm^2, and 5.9%, respectively. In the mode-locking operation, the mode-locked pulse train has a repetition rate of 16.6 MHz with pulse width of 24.2 ps. The laser wavelength is centered at 1992.9 nm with 3-dB spectrum width of 2.5 nm. The maximum output power is 110 mW with slope efficiency of 7.1%. Our experiment shows that $CsPbBr_3$ nanocrystal can be used as an efficient SA in the 2-μm wavelength region.

Keywords: nanocrystal, saturable absorber, mode-locking, fiber laser

PACS: 42.55.Wd, 42.60.Fc, 42.70.–a, 78.67.–n **DOI:** 10.1088/1674-1056/ab327c

1. Introduction

Passively mode-locked fiber lasers are widely applied in the fields of optical sensing, nonlinear frequency conversion, material processing, particle accelerating, and so on.[1–3] Compared with *Q*-switched operation, mode-locking can produce pulses with shorter pulse width, which makes it possible to achieve high peak power laser output. In real saturable absorber (SA) based passively mode-locked fiber lasers, the SA acts as a key photonic component with intensity dependent loss in the laser cavity, which transforms continuous wave to periodical laser pulse trains. Real SA-based ultrafast fiber lasers have attracted much attention because of their compactness, stability, and flexibility. Until now, many different kinds of materials have been explored and used as SAs in the ultrafast fiber laser field, such as semiconductor saturable absorber mirror (SESAM),[4] carbon nanotube (CNT),[5–8] graphene,[9] topological insulators,[10,11] transition metal dichalcogenides,[12–17] black phosphorus,[18,19] long-term stable group VA materials *X*ene (e.g., *X* = antimon,[20] bismuth[21]), flexible gold nanomaterials (e.g., gold nanorods,[22] gold nanostars,[23] gold nanobipyramids[24]), and so on.[25–31] Besides, zero-dimensional core–shell structures and two-dimensional layered van der Waals heterostructures are demonstrated to enhance the nonlinear optical modulation property.[32,33] So far, many different low-dimensional (including zero-, one-, and two-dimensional) nanomaterials have shown broadband (from visible to mid-infrared wavelength region) nonlinear optical response properties and great success has been achieved in ultrafast solid-sate and fiber lasers. For example, a CNT-based SA has been employed in a versatile multi-wavelength mode-locked fiber laser by Liu *et al.*[6] Because CNT is insensitive to environmental perturbation, they also revealed the entire buildup process of solitons and soliton molecules in mode-locked Er-doped fiber lasers by the use of CNT SA and time-stretch dispersive Fourier transform (TS DFT) technique in their work.[7,8] Although different kinds of nanomaterials have been used in pulsed lasers, they also suffer from some disadvantages, which restrict their further development in photonic and optoelectronic devices. CNT has a high optical damage threshold, but the scattering loss needs to be improved. SESAM has good nonlinear modulation property with narrow optical response bandwidth. Graphene has fast carrier mobility and broadband saturable absorption property (single layer absorption is $\sim 2.3\%$), but the modulation depth is low and the non-saturable loss should be improved. Topological insulators have gapless surface states, showing advantages of large modulation depth and third-order nonlinear susceptibility, however, the preparation process is relatively complicated. Black phosphorus has layer-dependent bandgap energy but accompanied with easy oxidation. So currently researchers are still exploring ideal nanomaterials that can be used in the ultrafast laser field.

All-inorganic colloidal nanocrystals of cesium lead halide perovskites $CsPbX_3$ (X = Cl, Br, I) have emerged as a new kind of optoelectronic material.[34,35] These perovskite nanocrystals show high photoluminescence quantum yield (up to 90%) and exhibit broad (400–700 nm) photoluminescence wavelength tunability through halide substitution and size

*Project supported by the National Key R&D Program of China (Grant No. 2018YFB0504500), the National Natural Science Foundation of China (Grant Nos. 51472162, 51672177, and 61475171), and the Talent Introduction Research Project of Shanghai Institute of Technology, China (Grant No. YJ 2018-8).

†Corresponding author. E-mail: fyz1003@sina.com

‡Corresponding author. E-mail: liaomeisong@siom.ac.cn

© 2019 Chinese Physical Society and IOP Publishing Ltd

control, which make them attractive in light emitting diode (LED) field. The third-order nonlinear optical properties of $CsPbX_3$ nanocrystals have also been explored in some previous work.[36,37] However, there have been few reports about their nonlinear absorption property in the 2-μm wavelength region.

In this paper, we report the nonlinear saturable absorption of $CsPbBr_3$ nanocrystal in the 2-μm wavelength region. The modulation depth and saturable intensity were measured to be ~ 14.1% and 2.5 MW/cm^2, respectively. Then we employed it as SA to passively mode-lock a Tm-doped fiber laser in a ring cavity. Our experiment shows that $CsPbBr_3$ nanocrystal can be an efficient SA for 2-μm pulsed fiber laser.

2. Experiment

The fabrication process of $CsPbBr_3$ nanocrystal has been described in detail in our previous paper.[26] The linear optical absorption spectrum of $CsPbBr_3$ nanocrystal from 300 nm to 2500 nm (1 nm resolution) is shown in Fig. 1. We can see that it has steady absorption from 300 nm to 600 nm. Then the absorption drops dramatically near 800 nm, which is due to its bandgap. And it has relatively low absorption at the 2-μm wavelength region compared with that at the visible light region. The moderate absorption at the 2-μm wavelength region may be caused by edge states and crystallographic defects of the $CsPbBr_3$ nanocrystal film. The inset in Fig. 1 is the corresponding SEM image of $CsPbBr_3$ nanocrystal, indicating that the nanocrystal size is near 20 nm.

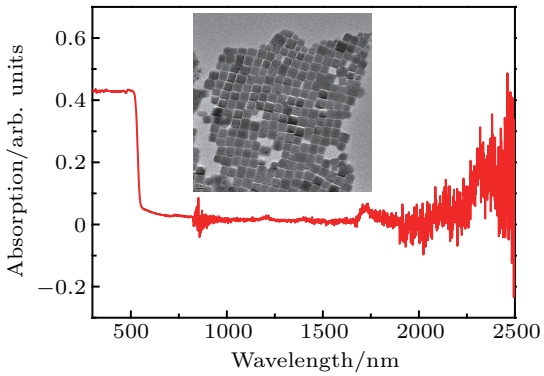


Fig. 1. Linear absorption spectrum of $CsPbBr_3$ nanocrystal from 300 nm to 2500 nm. The inset is the SEM image of $CsPbBr_3$ nanocrystal, the black label is 20 nm.

We fabricated $CsPbBr_3$ SA by drop coating the corresponding toluene liquid solution on a gold mirror and dried it at room temperature to form a $CsPbBr_3$ nanocrystal film. The mirror covered with the film acts as a reflective saturable absorption mirror in the laser experiment, and it is different from the transmission type SA which is sandwiched between two fiber connectors, such as in Refs. [6]–[8]. After that, we used a reflection method to investigate the nonlinear absorption property of the $CsPbBr_3$ nanocrystal SA. A home-made mode-locked fiber laser (central wavelength ~ 2010 nm, pulse width ~ 80 ps, repetition rate ~ 55.6 MHz) was used as the pump source. The reflected output power was measured with a power meter (Thorlabs) with increased incident probe power. The experimental setup of the nonlinear absorption measurement is shown in Fig. 2(a), and the incident probe power could be varied through rotating a $\lambda/2$ plate. The experimental data were fitted with the equation $R = 1 - \alpha_0 \exp(-I/I_{sat}) - \alpha_{ns}$, where R is the reflection of the pulsed laser, α_0 is the modulation depth, I is the incident probe intensity, I_{sat} is the saturable intensity, and α_{ns} is the non-saturable loss. The corresponding result is shown in Fig. 2(b). We can see that the modulation depth, saturable intensity, and non-saturable loss are 14.1%, 2.5 MW/cm^2, and 5.9%, respectively.

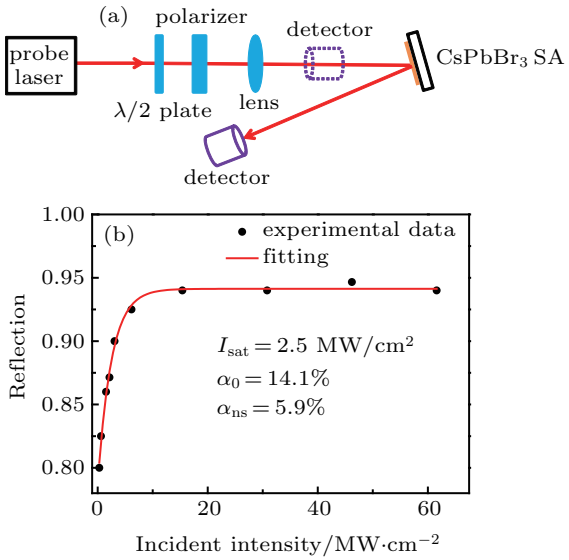


Fig. 2. (a) Experimental setup of the nonlinear absorption measurement, (b) nonlinear saturable absorption property of $CsPbBr_3$ nanocrystal.

The laser mode-locking experiment setup is shown in Fig. 3. A fiber ring cavity is adopted to achieve passive mode-locking. The pump source is a 7 W 793 nm laser diode (BWT). The pump laser is coupled into the cavity through a fiber combiner (ITF), then absorbed by ~ 3 m Tm-doped double-clad fiber (Nufern, SM-TDF-10P/130-HE, absorption of 3 dB/m @793 nm). Other fibers in the cavity are all single-mode fibers (SMF-28e). The group-velocity dispersion (GVD) of Tm fiber and SMF-28e fiber are −130 ps^2/km and −78 ps^2/km, respectively. The total cavity length is ~ 12 m and the net cavity dispersion is −1.092 ps^2. The 2-μm laser travels unidirectionally in the cavity with the aid of a circulator (AFR). $CsPbBr_3$ nanocrystal SA is placed at port 2 of the circulator, so laser passes through the $CsPbBr_3$ nanocrystal SA twice (1→ 2 → SA→ 2 → 3) in every trip. A fiber coupler (AFR) is used to output laser every roundtrip with 20% ratio. Because most of pump power is absorbed by the Tm-doped fiber, and the residual is absorbed by pigtails' clad of the circulator at port 2, there is negligible pump power entering the circulator and reaching

the SA. A polarization controller (PC) placed in the cavity is for the control of intra-cavity birefringence.

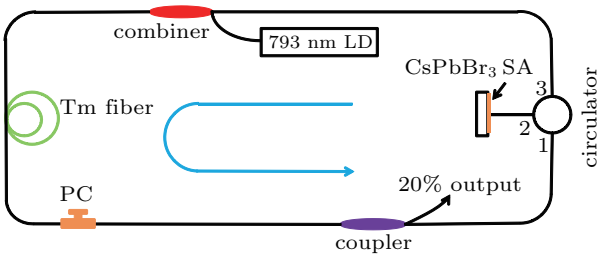


Fig. 3. Experimental setup of mode-locked Tm-doped fiber laser with $CsPbBr_3$ nanocrystal SA.

In the experiment, the laser output power was measured with a power meter (Thorlabs). The optical spectrum was detected with a spectrometer (Sandhouse). The single pulse waveform was measured with a commercial autocorrelator (APE). A 2.5 GHz oscilloscope (Agilent) was combined with a photodetector (Newport, 1 GHz) to real-time monitor the temporal pulses. The radio frequency (RF) spectrum was measured by combining the photodetector with a frequency spectrum analyzer (CETC-41).

In the experiment, stable mode-locked pulses occurred at pump power $\sim$ 1.9 W when we carefully rotated the PC. Figure 4 shows the mode-locking result. Figure 4(a) is the recorded pulse train with a pulse interval of 62 ns, which corresponds to $\sim$ 12 m cavity length. The pulse train has some noise, which may be due to environmental perturbation (e.g., temperature and air flow) or randomly distributed birefringence in the ring fiber cavity. Figure 4(b) is the RF spectrum of the laser pulses, showing 36.3 dB signal-to-noise ratio (SNR) of the fundamental frequency at 16.6 MHz with 500 Hz resolution. The SNR can be improved through optimizing the fabrication process of the $CsPbBr_3$ nanocrystal SA film, or other cavity parameters like cavity birefringence, cavity loss, and output coupling ratio. The single pulse waveform was measured with an autocorrelator and it shows that the pulse width is 24.2 ps. The laser wavelength in Fig. 4(d) was measured with 0.15 nm resolution and the central wavelength is 1929.9 nm with 3-dB bandwidth of 2.5 nm. The mode-locked pulses that work in the anomalous dispersion region have no Kelly sidebands, thus we suspect that the mode-locking stability is not high enough (SNR$<$ 40 dB) to achieve resonant coupling between the soliton and dispersive waves. The time-bandwidth product was calculated to be 4.9, showing relatively high chirp in the cavity. The high chirp may be caused by the high fiber nonlinearity (or self-phase modulation) experienced by laser pulses in the fiber ring cavity.

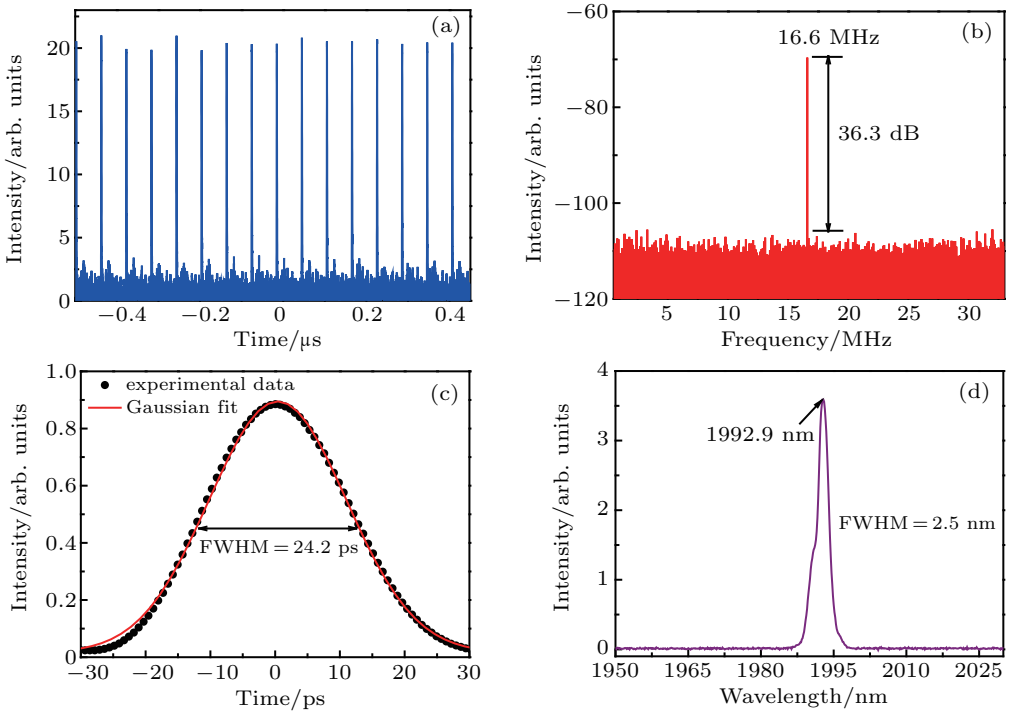


Fig. 4. Mode-locking result of Tm-doped fiber laser: (a) pulse train, (b) radio frequency spectrum, (c) single pulse waveform, and (d) optical spectrum.

The relationship between the pump power and output power is described in Fig. 5(a). Continuous wave mode-locking appears at pump power $\sim$ 1.9 W, then the output power has linear increase with the pump power. The output power reaches $\sim$ 110 mW at the pump power of 3.44 W. The slope efficiency is 7.1% with linear fitting, and may have space to be improved with more careful cavity designs, such as the length of the gain fiber, the output ratio, and the modulation depth of the SA. Figure 5(b) shows the stability measurement of the mode-locking state at the maximum output power within 1 h.

We can see that in the first half hour, the output power is almost unchanged, but in the second half hour it has ~ 6% power fluctuation without losing mode-locking state, which may be due to the thermal effect of the $CsPbBr_3$ nanocrystal SA at high power laser output. It should be mentioned that the fabricated $CsPbBr_3$ nanocrystal SA can work for several months in mode-locking experiment, with no obvious degrading of the output laser properties.

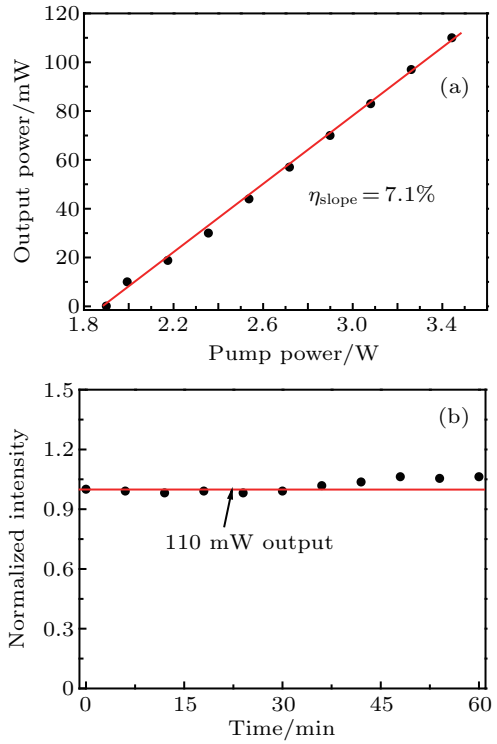


Fig. 5. (a) Relationship between pump power and output power, (b) stability measurement in 1 h.

3. Conclusion

In this paper, we have successfully prepared $CsPbBr_3$ nanocrystal SA, and used it to passively mode-lock a Tm-doped fiber laser. The $CsPbBr_3$ nanocrystal SA has modulation depth, saturable intensity, and non-saturable loss of 14.1%, 2.5 MW/cm^2, and 5.9%, respectively. In the mode-locking operation, the pulse repetition rate is 16.6 MHz with 24.2 ps pulse width. The laser wavelength is centered at 1929.9 nm with 2.5 nm 3-dB width. The maximum output power is 110 mW without damaging the SA. Our experiment shows that $CsPbBr_3$ nanocrystal can be an efficient SA for the 2-μm wavelength region, and has potential to be a candidate in high power mode-locking fiber laser oscillators.

References

[1] Keller U 2003 *Nature* **424** 831
[2] Grelu P and Akhmediev N 2012 *Nat. Photon.* **6** 84
[3] Mourou G, Brocklesby B, Tajima T and Limpert J 2013 *Nat. Photon.* **7** 258
[4] Lin H F, Zhang G, Zhang L Z, Lin Z B, Pirzio F, Agnesi A, Petrov V and Chen W D 2017 *Opt. Mater. Express* **7** 3791
[5] Li W S, Zhu C H, Rong X F, Wu J J, Xu H Y, Wang F Q, Luo Z C and Cai Z P 2018 *J. Lightwave Technol.* **36** 2694
[6] Liu X M, Han D D, Sun Z P, Zeng C, Lu H, Mao D, Cui Y D and Wang F Q 2013 *Sci. Rep.* **3** 2718
[7] Liu X M, Yao X K and Cui Y D 2018 *Phys. Rev. Lett.* **121** 023905
[8] Liu X M and Cui Y D 2019 *Adv. Photon.* **1** 016003
[9] Sun Z P, Hasan T, Torrisi F, Popa D, Privitera G, Wang F Q, Bonaccorso F, Basko D M and Ferrari A C 2010 *ACS Nano* **4** 803
[10] Luo Z C, Liu M, Liu H, Zheng X W, Luo A P, Zhao C J, Zhang H, Wen S C and Xu W C 2013 *Opt. Lett.* **38** 5212
[11] Lee J and Lee J H 2018 *Chin. Phys. B* **27** 094219
[12] Zhang H, Lu S B, Zheng J, Du J, Wen S C, Tang D Y and Loh K P 2014 *Opt. Express* **22** 7249
[13] Kadir N A A, Ismail E I, Latiff A A, Ahmad H, Arof H and Harun S W 2017 *Chin. Phys. Lett.* **34** 014202
[14] Mao D, Cui X Q, Gan X T, Li M K, Zhang W D, Lu H and Zhao J L 2018 *IEEE J. Sel. Top. Quantum Electron.* **24** 1100406
[15] Liu M L, Ouyang Y Y, Hou H R, Lei M, Liu W J and Wei Z Y 2018 *Chin. Phys. B* **27** 084211
[16] Luo Z C, Liu M, Luo A P and Xu W C 2018 *Chin. Phys. B* **27** 094215
[17] Zhang R L, Wang J, Zhang X Y, Lin J T, Li X, Kuan P W, Zhou Y, Liao M S and Gao W Q 2019 *Chin. Phys. B* **28** 014207
[18] Lu S B, Miao L L, Guo Z N, Qi X, Zhao C J, Zhang H, Wen S C, Tang D Y and Fan D Y 2015 *Opt. Express* **23** 11183
[19] Liu M, Jiang X F, Yan Y R, Wang X D, Luo A P, Xu W C and Luo Z C 2018 *Opt. Commun.* **406** 85
[20] Luo H Y, Tian X L, Gao Y, Wei R F, Li J F, Qiu J R and Liu Y 2018 *Photon. Res.* **6** 900
[21] Guo B, Wang S H, Wu Z X, Wang Z X, Wang D H, Huang H, Zhang F, Ge Y Q and Zhang H 2018 *Opt. Express* **26** 22750
[22] Luo H Y, Kang Z, Gao Y, Peng H L, Li J F, Qin G S and Liu Y 2019 *Opt. Express* **27** 4886
[23] Yang L L, Kang Z, Huang B, Li J, Miao L L, Tang P H, Zhao C J, Qin G S and Wen S C 2018 *Opt. Lett.* **43** 5459
[24] Zhang H N and Liu J 2016 *Opt. Lett.* **41** 1150
[25] Zhou Y, Zhao M, Wang S W, Hu C X, Wang Y, Yan S, Li Y, Xu J Q, Tang Y L, Gao L F, Wang Q and Zhang H L 2016 *Opt. Lett.* **41** 1221
[26] Zhou Y, Hu Z P, Li Y, Xu J Q, Tang X S and Tang Y L 2016 *Appl. Phys. Lett.* **108** 261108
[27] Muhammad A R, Ahmad M T, Zakaria R, Rahim H R A, Yusoff S F A Z, Hamdan K S, Yusof H H M, Arof H and Harun S W 2017 *Chin. Phys. Lett.* **34** 034205
[28] Aziz N A, Latiff A A, Lokman M Q, Hanafi E and Harun S W 2017 *Chin. Phys. Lett.* **34** 044202
[29] Fu S G, Ouyang X Y, Li J J and Liu X J 2017 *Chin. Phys. Lett.* **34** 044203
[30] Lv R D, Li L, Wang Y G, Chen Z D, Liu S C, Wang X, Wang J and Li Y F 2018 *Chin. Phys. B* **27** 114214
[31] Sun Y J, Tu C Y, You Z Y, Liao J S, Wang Y Q and Xu J L 2018 *Opt. Mater. Express* **8** 165
[32] Ming N, Tao S N, Yang W Q, Chen Q Y, Sun R Y, Wang C, Wang S Y, Man B Y and Zhang H N 2018 *Opt. Express* **26** 9017
[33] Liu W J, Zhu Y N, Liu M L, Wen B, Fang S B, Teng H, Lei M, Liu L M and Wei Z Y 2018 *Photon. Res.* **6** 220
[34] Wang Y, Li X M, Song J Z, Xiao L, Zeng H B and Sun H D 2015 *Adv. Mater.* **27** 7101
[35] Protesescu L, Yakunin S, Bodnarchuk M I, Krieg F, Caputo R, Hendon C H, Yang R X, Walsh A and Kovalenko M V 2015 *Nano Lett.* **15** 3692
[36] Wang Y, Li X M, Zhao X, Xiao L, Zeng H B and Sun H D 2016 *Nano Lett.* **16** 448
[37] Krishnakanth K N, Seth S, Samanta A and Rao S V 2018 *Opt. Lett.* **43** 603